Journal of Hazardous Materials 246–247 (2013) 189–198

Contents lists available at SciVerse ScienceDirect

Journal of Hazardous Materials

journal homepage: www.elsevier.com/locate/jhazmat

Response of magnetic properties to heavy metal pollution in dust from three industrial cities in China

Zongmin Zhu[a,*], Zhonggen Li[b], Xiangyang Bi[a], Zhixuan Han[c], Genhua Yu[a]

[a] State Key Laboratory of Biogeology and Environmental Geology, China University of Geosciences, Wuhan 430074, China
[b] State Key Laboratory of Environmental Geochemistry, Institute of Geochemistry, Chinese Academy of Sciences, Guiyang 550002, China
[c] Institute of Geophysical and Geochemical Exploration, Langfang 065000, China

HIGHLIGHTS

- Elevated magnetic particles and heavy metals coexist in dust.
- Morphology and mineralogy of magnetic particles were studied by SEM-EDX and XRD.
- Magnetic minerals in the dust consist of magnetite, hematite, and metallic iron.
- Impact of metallic iron particles and multi-sources of metal pollutants was notable.

ARTICLE INFO

Article history:
Received 15 October 2012
Received in revised form
10 December 2012
Accepted 11 December 2012
Available online 20 December 2012

Keywords:
Environmental magnetism
Heavy metals
Dust
Non-ferrous metal industries

ABSTRACT

Magnetic method is a reliable and powerful technique for identification of the relative contribution of industrial pollutants. However, it has not been fully applied in urban area impacted by non-ferrous metal (NFM) smelting/processing activities. The aim of this study is to explore the applicability of magnetic methods for detecting heavy metal contamination in dust from three NFM smelting/processing industrial cities (Ezhou, Zhuzhou, and Hezhang) in China. The enhancements of magnetic susceptibility (MS) and saturation isothermal remanent magnetization (SIRM) together with heavy metals were significant in the studied areas in comparison with the background values. Scanning electron microscope (SEM) analysis revealed that magnetic particles in dust from Ezhou were dominated by spherules, while those from Zhuzhou and Hezhang were mainly consisted of irregular-shaped particles. κ–T curves and X-ray diffraction (XRD) analyses indicated that the magnetic particles from Ezhou were dominated by magnetite and metallic iron, whereas those from Zhuzhou and Hezhang were consisted of magnetite and hematite. Our study indicates that magnetic properties of the dust are sensitive to the NFM smelting/processing related heavy metal pollutants. However, the relationship between magnetic parameters and heavy metals was influenced by the presence of metallic iron particles and multi-sources of metal pollutants.

1. Introduction

Environmental contamination of heavy metals is still a serious problem in urban areas due to the constant release of metal pollutants from various industrial operations, traffic emissions, power generation facilities, fossil fuel burning, and municipal waste disposal. Heavy metals emitted from anthropogenic sources are generally accompanied with emissions of ferromagnetic/ferrimagnetic particles. In addition, iron hydroxides/oxides are excellent absorbers and carriers of heavy metals, due to their large specific surface area. Therefore, the contaminated extent and toxicity of heavy metals can be revealed by magnetic measurement (e.g., magnetic susceptibility and saturation isothermal remanence), which is considered to be a simple, rapid, low-cost, and non-destructive method. In recent decades, magnetic approach has been successfully applied to quantifying the levels of heavy metals in various environmental samples, including soils [1–6], road dusts [7–12], sediments or sludge [13–18], and tree leaves or mosses [1,19–23]. The published environmental magnetic studies have mainly focused on heavy metal contamination by iron and steel smelting activities, coal-fired power plants, and traffic emissions. However, reports on the application of magnetic properties to studying the environmental pollution of non-ferrous metal (NFM) smelting/processing and related activities were sparse, despite the fact that they (especially Zn/Pb smelting) have long been

* Corresponding author. Tel.: +86 27 67883001; fax: +86 27 67883002.
E-mail address: zhumin@cug.edu.cn (Z. Zhu).

0304-3894/$ – see front matter © 2012 Elsevier B.V. All rights reserved.
http://dx.doi.org/10.1016/j.jhazmat.2012.12.024

recognized as one of the most important local sources of metallic pollution.

Urban dust, consisted of soil, deposited airborne particulate, soot and fume discharged from various industries and vehicles and so on, is an important media which hosts environmental pollutants. Through resuspension–inhalation, hand-mouth ingestion and dermal contact, hazardous pollutants contained in urban dust could enter human bodies and endanger human's health [24–27]. Therefore, the development of rapid and efficient monitoring systems to study the concentration and distribution of heavy metals in urban dust will help mitigate the effects of urban pollution on public health [20].

In the present study, we investigated magnetic properties and heavy metal concentrations in urban dust from three typical industrial areas in China, which might have been contaminated predominantly by NFM smelting/processing and related activities. The aims of this research are (1) to determine the magnetic characteristics of urban dust impacted by NFM smelting/processing and related activities, and (2) to explore if there is a possible relationship between the enhanced concentrations of NFM smelting/processing related magnetic minerals and heavy metals.

2. Materials and methods

2.1. Studied areas and sample collection

In this study, ground deposited dust samples were collected from three typical industrial cities in China, which were Zhuzhou city in Hunan province, Ezhou city in Hubei province, and Hezhang city in Guizhou province. Zhuzhou (112°57′–114°07′E, 26°03′–28°01′N) is located at eastern Hunan province with a population of 3.85 million and an area of 11,262 km^2. Zhuzhou is one of the largest lead and zinc producers in Asia. Lead and Zn are smelted using traditional pyrometallurgical and hydrometallurgical methods. In addition, this city also has some smelting related industries, such as hard alloy plants. Hezhang city (104°10′–105°03′E, 26°46′–27°28′N) is situated at about 340 km west of Guiyang, the capital of Guizhou Province. It lies on the Yunnan–Guizhou Plateau (1230–2900 m above sea level) with a population of 0.69 million and an area of 3245 km^2. Artisanal zinc smelting using indigenous methods had been widely applied in this area since the 17th century. Ezhou (114°32′–115°05′E, 30°00′–30°06′N) is located at eastern Hubei province with a population of 1.07 million and an area of 1505 km^2. Ezhou is a relatively small scale industry city which had been impacted by historical copper and iron smelting and processing activities. Furthermore, small steel and NFM (copper and aluminum alloys) processing plants are widespread in this studied area.

Dust samples were collected at the edges of main roads with an interval of 500–1000 m between sampling sites from the main urban areas of the studied cities. At each sampling site, 50–100 g dust was sampled within an area of about 2 m × 2 m using a brush and plastic spatula, stored in polyethylene bags, and then transported to the laboratory. In total 43, 26, and 22 road dust samples were taken from Zhuzhou, Hezhang, and Ezhou, respectively. In order to assess the contamination extent of the NFM smelting/processing activities, relatively uncontaminated soil dusts from each of the studied cities were also collected as background samples for comparison.

In the laboratory, the dust samples were air-dried at room temperature, and passed through a 1.0 mm sieve to remove rocks, plants, hair and other impurities. The homogenized dust samples were ground to a fine powder texture with an agate mortar prior to chemical analyses.

2.2. Experimental methods

Bulk magnetic susceptibility (κ) of the dust was measured with a kappabridge KLY-3 (AGICO, Brno) at 875 Hz operating frequency and 300 Am^{-1} field intensity, and it was calculated as mass susceptibility (s) in 10^{-8} m^3/kg. Magnetic susceptibility (MS) at low (χ_{lf}, 976 Hz) and high (χ_{hf}, 15,616 Hz) frequencies were measured with a kappabridge MFK1-FA (AGICO, Brno) at 200 Am^{-1} field intensity. Frequency-dependent susceptibility (χ_{fd}%) was then calculated and expressed as a percentage $\chi_{fd}\% = (\chi_{lf} - \chi_{hf})/\chi_{lf} \times 100\%$. An isothermal remanent magnetization (IRM) experiment was performed with an ASC Scientific (Model IM-10) impulse magnetizer and Molspin magnetometer. The IRM acquired in a field of 1.0 T was regarded as saturation IRM (SIRM). The temperature-dependence of the low-field magnetic susceptibility curve of typical dust samples was conducted with a Kappabridge KLY-4 equipped with a CS-4 high temperature furnace in an argon atmosphere.

After obtaining the magnetic measurements of the bulk samples, the magnetic particles were separated from the dust samples using a hand magnet and were used for morphology and mineralogy analysis. The χ and SIRM were measured before and after the magnetic extractions to evaluate the extraction efficiency [7,28]. The χ and SIRM values of the magnetic extracts were found to be >96% of those before extraction, indicating that the magnetic particles in the dusts were effectively separated. For morphology analysis, the extracts were fixed by gum and covered by a gold layer, and then analyzed with an environmental Scanning Electron Microscope (SEM) (Model Quanta 200) equipped with an energy dispersive X-ray spectrometer (EDX) microanalyzer (analytical condition of 20 kv of accelerating voltage and 2×10^{-9} A of beam current). Mineralogy of the magnetic extracts was characterized using a powder X-ray diffractometer (XRD) (X' Pert PRO DY2198, PANalytical Inc.). The diffraction pattern was recorded from 3° to 65°.

About 0.25 g of the prepared dust sample was digested with a concentrated HNO_3–$HClO_4$–HF–HCl mixture. The concentrations of common heavy metals of the digested solution were determined by an inductively coupled plasma-atomic emission spectrometer (ICP-AES). QA/QC included reagent blanks, analytical duplicates, and analysis of the standard reference material (SRM) (SRM 2704 and 1648). The recovery rates for the considered metals in the SRM were between 75 and 115%.

2.3. Statistical analysis

The data were statistically analyzed using the statistical package, SPSS v13.0 (SPSS Inc.). A one-way ANOVA test ($p < 0.05$) was used to analyze the difference in analytical results among different sampling sites. The correlation analysis between magnetic parameters and metal concentrations was conducted by a Pearson correlation, and the level of significance was set at $p < 0.05$ and $p < 0.01$ (two-tailed).

Pollution assessment for single heavy metal was conducted using geoaccumulation index (I_{geo}) introduced by Müller [29], which is calculated using the following equation:

$$I_{geo} = \log_2 \left[\frac{C_{m\text{Sample}}}{(1.5 \times C_{m\text{Background}})} \right] \quad (1)$$

where $C_{m\text{Sample}}$ is the measured concentration of the metal in dust, $C_{m\text{Background}}$ is the geochemical background value. The factor 1.5 is introduced in this equation to minimize the effect of possible variations in the background values. According to Muller [29], the I_{geo} for each metal is calculated and classified as: uncontaminated ($I_{geo} \leq 0$); uncontaminated to moderately contaminated ($0 < I_{geo} \leq 1$); moderately contaminated ($1 < I_{geo} \leq 2$); moderately to heavily contaminated ($2 < I_{geo} \leq 3$); heavily contaminated

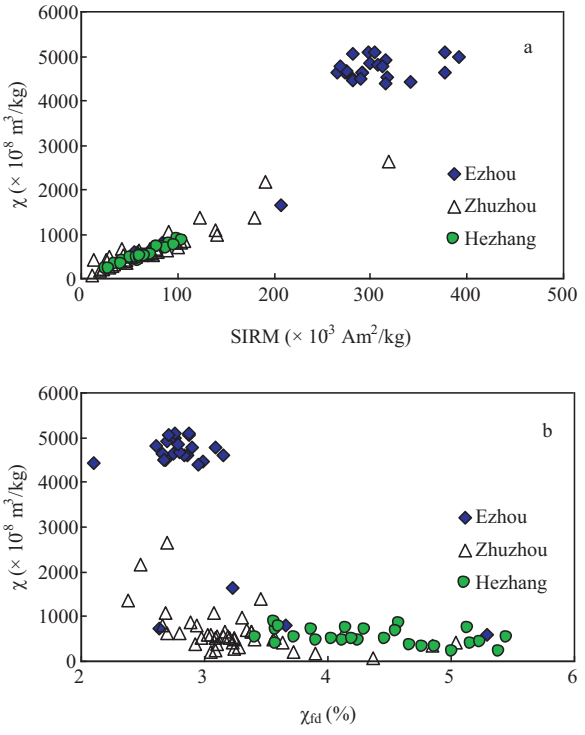

Fig. 1. Correlation scatter diagram between χ and SIRM (a) and between χ and χ_{fd} (b) in dust.

($3 < I_{geo} \leq 4$); heavily to extremely contaminated ($4 < I_{geo} \leq 5$); extremely contaminated ($I_{geo} \geq 5$).

In order to assess the integrative impact of anthropogenic activity related heavy metals, the Tomlinson pollution load index (PLI) was calculated based on each of the metal concentrations (Fe, Mn, As, Ba, Cd, Co, Cr, Cu, Ni, Pb, V, and Zn) [30]. The PLI index is defined as the nth root of the multiplication of the concentration factors (CF):

$$\mathrm{PLI} = \sqrt[n]{(CF_1 \times CF_2 \times CF_3 \times \cdots CF_n)} \quad (2)$$

where CF is the ratio between the concentration of each heavy metal and its corresponding background value. According to Singh et al. [31], the PLI was classified as: $0 < \mathrm{PLI} \leq 1$ unpolluted; $1 < \mathrm{PLI} \leq 2$ moderately to unpolluted; $2 < \mathrm{PLI} \leq 3$ moderately polluted; $3 < \mathrm{PLI} \leq 4$ moderately to highly polluted; $4 < \mathrm{PLI} \leq 5$ highly polluted; $\mathrm{PLI} > 5$ very highly polluted.

3. Results and discussion

3.1. Magnetic parameters and heavy metals

The summary of basic magnetic parameters, including χ, SRIM and χ_{fd}%, and heavy metal concentrations of the dust samples are listed in Table 1. Dust samples from Ezhou had extremely high values of χ, which varied from 593 to $5098 \times 10^{-8}\ m^3/kg$ with a mean of $4150 \times 10^{-8}\ m^3/kg$, while the levels of χ in dust from Zhuzhou (mean $663 \times 10^{-8}\ m^3/kg$) and Hezhang (mean $527 \times 10^{-8}\ m^3/kg$) were significantly lower. Similarly, the highest values of SIRM were consistently found in the samples from Ezhou (mean $276 \times 10^{-3}\ Am^2/kg$). These enhanced magnetic results clearly indicate the serious impact of NFM smelting and processing activities on the ambient environment. There was a significant correlation between SIRM and χ in dust from the three areas ($r^2 = 0.829 \sim 0.954$, $p < 0.001$) (Fig. 1a), indicating that ferrimagnetic phases are the dominant magnetic minerals in the dust samples [32]. But this linear correlation from Ezhou was less

Table 1
Summary of magnetic properties and heavy metal concentrations of dust.

	Ezhou ($n = 22$)[a]				Zhuzhou ($n = 43$)				Hezhang ($n = 26$)			
	Range	Median	Mean ± SD	BV[b]	Range	Median	Mean ± SD	BV	Range	Median	Mean ± SD	BV
χ ($\times 10^{-8}$ m^3/kg)	593–5098	4620	4150 ± 1420	74	79–2642	546	663 ± 485	65	199–864	496	527 ± 182	83
SIRM ($\times 10^{-3}$ Am^2/kg)	55–391	292	276 ± 84	12	11–319	60	74 ± 56	11	25–106	65	66 ± 22	13
χ_{fd} (%)	2.1–5.3	2.8	2.9 ± 0.01	5.5	2.4–5.0	3.2	3.3 ± 0.5	4.4	3.4–5.5	4.3	4.4 ± 0.6	8.8
Fe (g/kg)	35–214	152	142 ± 39	21	15–102	34	36 ± 14	15	26–62	42	42 ± 8.7	29
Mn (g/kg)	0.83–15	8.0	7.6 ± 2.9	0.34	0.32–7.2	0.98	1.2 ± 1.1	0.32	0.39–1.0	0.76	0.73 ± 0.14	0.57
As (mg/kg)	11–30	20	20 ± 4.0	12	11–361	46	61 ± 62	14	28–81	56	56 ± 12	10
Ba (mg/kg)	570–1860	650	743 ± 570	321	240–1000	430	456 ± 157	310	140–430	290	289 ± 67	270
Cd (mg/kg)	0.80–1.8	1.4	1.4 ± 0.24	0.22	4.6–202	15	27 ± 38	0.28	2.9–20	5.8	6.7 ± 3.5	0.3
Co (mg/kg)	10–198	78	76 ± 34	6.0	7.0–76	13	15 ± 11	7.0	8.0–19	14	14 ± 2.7	7.0
Cr (mg/kg)	101–15,000	9580	8790 ± 3460	52	32–366	111	127 ± 64	32	65–132	99	96 ± 17	76
Cu (mg/kg)	48–1740	853	822 ± 346	16	29–549	125	158 ± 111	29	48–362	94	112 ± 65	42
Ni (mg/kg)	23–2870	1050	1030 ± 522	14	12–67	35	37 ± 12	12	22–58	35	36 ± 8.6	18
Pb (mg/kg)	66–2800	351	424 ± 494	28	115–3860	370	541 ± 671	32	175–809	395	416 ± 142	47
V (mg/kg)	62–158	113	111 ± 19	46	35–101	56	57 ± 14	36	63–122	103	97 ± 15	52
Zn (mg/kg)	256–1130	827	810 ± 157	69	506–10,000	1380	2210 ± 2100	51	640–2320	1070	1090 ± 363	132
PLI	2.1–23	12	12 ± 4.1		1.8–11	4.3	5.0 ± 2.0		1.8–4.5	2.9	2.9 ± 0.64	

[a] Not counting the background samples.
[b] Background value.

significant than those from Zhuzhou and Hezhang (Fig. 1a), which might be attributed to the presence of ferromagnetic minerals (i.e., metallic iron) in these samples because the contributions of metallic iron to the intensity of SIRM and χ are different from the ferrimagnetic minerals (magnetite) [33].

Frequency-dependent magnetic susceptibility (χ_{fd}%) is sensitive to the superparamagnetic (SP) component and thus can provide information on the relative contribution of SP magnetite grains in the material. If χ_{fd}% > 4%, the assemblage of magnetic grains contains a significant portion of SP particles, whereas χ_{fd}% < 4% indicates a low proportion of SP particles [34]. Dust samples from Ezhou and Zhuzhou had mean χ_{fd}% values of 2.9 and 3.3%, respectively, which suggests that magnetic carriers in these samples are predominately coarse-grained particles and the proportion of SP particles is much low. However, dust from Hezhang had relatively higher values of χ_{fd}% (mean 4.4%), which may reflect the presence of a mixture of pedogenic ferromagnetic particles, which are indicated to be very fine grains (SP), combined with larger anthropogenic ones [1]. A clear trend of increasing χ_{fd}% with decreasing χ was found in dust from the studied areas (Fig. 1b), which suggested that the coarse anthropogenic particles dominated the χ in the dust.

Consistent with the enhanced magnetic parameters, heavy metal concentrations in dusts from the NFM smelting/processing industrial cities were significantly elevated in comparison with the background values (Table 1). The highest mean concentrations of Fe (142 g/kg), Mn (7.6 g/kg), Ba (743 mg/kg), Co (76 mg/kg), Cr (8790 mg/kg), Cu (822 mg/kg), Ni (1030 mg/kg), and V (111 mg/kg) were consistently found in Ezhou, whereas higher concentrations of As, Cd, and Zn were found in Zhuzhou and Hezhang. The contamination situation of each metal can be clearly reflected by the geoaccumulation index (I_{geo}) (Fig. 2). With regard to dust from Ezhou, Cr, Ni, Cu, and Mn showed high values of I_{geo} (mean 3.7–6.2), representing heavily contaminated to extremely contaminated, while an uncontaminated to moderately contaminated status was found for V, Ba, and As ($I_{geo} = 0.12 \sim 0.67$). For Zhuzhou and Hezhang, the major metal pollutants were Cd, Zn, and Pb, which revealed a contaminated status of between moderately to heavily contaminated and extremely contaminated ($I_{geo} = 2.4–5.3$). On the contrary, the contamination of Ni, Fe, Co, V, and Ba in these cities were less serious ($I_{geo} < 1$). The Tomlinson pollution load index (PLI) reveals the integrative contamination of the whole metal pollutants. As shown in Table 1, dust from Ezhou had the highest PLI (mean 12), revealing a very high pollution. On the other hand, dusts from Zhuzhou had been highly polluted (mean PLI = 5.0) and those from Hezhang had been moderately polluted (mean PLI = 2.9) by the considered heavy metals.

Magnetic parameters and heavy metals in dust of this study were compared with those in other cities around the world (Table 2) [8,12,35–39]. The mean concentrations of χ, SIRM, and heavy metals in Ezhou were significantly higher than those in both the industrial city (Loudi) [35] and most common cities [8,12,35–39]. Meanwhile, the data in Zhuzhou and Hezhang were higher (or similar) than those in most of the listed common cities [8,12,36,38], except Zn in Hong Kong [37] and Pb and Zn in Liverpool [39]. This comparison indicates that the contribution of the NFM smelting/processing industries to the enhancement of magnetic minerals and heavy metals is obvious, and the coexistence of elevated magnetic minerals and heavy metals is a common phenomenon in both industrial and common cities.

3.2. Magnetic mineralogy

Magnetic mineralogy was analyzed for three representative dust samples (one sample from each of the studied cities), which were collected near the industrial emission sources and had typical values of magnetic parameters and heavy metal concentrations

Table 2
Comparison of magnetic parameters and heavy metals in dust of different cities.

Cities	χ ($\times 10^{-8}$ m^3/kg)	SIRM ($\times 10^{-3}$ Am^2/kg)	Fe (g/kg)	Mn (g/kg)	Cd (mg/kg)	Co (mg/kg)	Cr (mg/kg)	Cu (mg/kg)	Ni (mg/kg)	Pb (mg/kg)	Zn (mg/kg)	References
Ezhou (China)	4150	276	142	7.6	1.4	76	8790	822	1030	424	810	This study
Zhuzhou (China)	663	74	36	0.98	27	15	127	158	37	541	1380	This study
Hezhang (China)	527	66	42	0.76	6.7	14	96	112	36	416	1070	This study
Wuhan (China)	132	119	32	0.60	–	12	75	62	28	103	224	8
Lanzhou (China)	442	66	34	0.59	–	–	62	73	–	63	297	12
Loudi (China)	880	211	93	–	2.2	19	225	141	49	228	583	35
Xi'an (China)	487	–	31	–	–	–	96	83	–	104	291	36
Hong Kong (China)												
Causeway Bay	637	86	10	0.42	5.4	–	69	442	–	46	3827	37
Sandy Bay	404	50	12	0.38	1.2	–	67	175	–	55	2319	37
Seoul (Korea)	62	73	19	0.44	–	–	151	396	–	144	795	38
Liverpool (U.K.)	503	61	44	–	–	–	–	–	–	892	1470	39

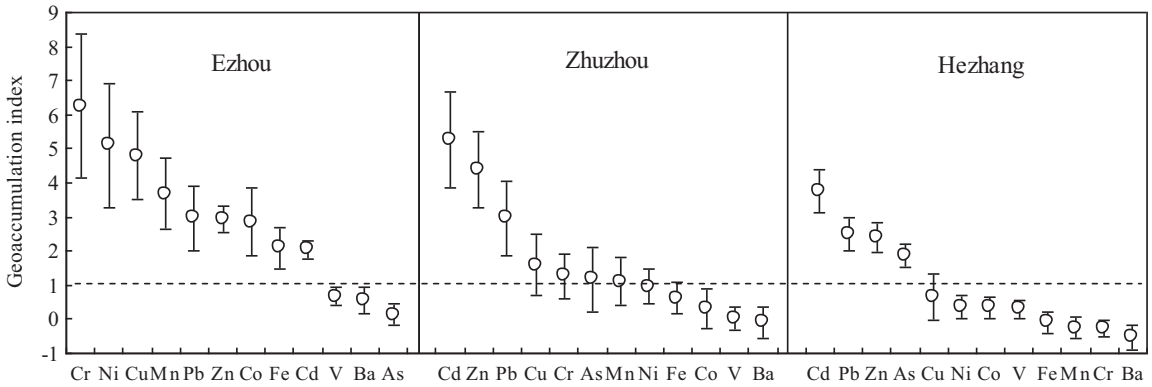

Fig. 2. Geoaccumulation index (I_{geo}) of heavy metals in dust.

(close to the mean of each data set). IRM acquisition and back-field demagnetization curves are shown in Fig. 3. The measured samples rapidly acquired IRM at low fields (<100 mT) and near saturation at ~300 mT (>90%), whilst back-field demagnetization curves displayed a softer behavior with Bcr values less than 50 mT. This pattern indicates a predominance of low-coercivity Fe-oxides (e.g., Fe_3O_4) [7]. This finding can be further supported by the temperature-dependent susceptibility (κ–T) cycles (Fig. 4). The thermomagnetic behavior for all samples showed a Curie temperature (T_C) at about 580 °C, revealing the presence of magnetite as the dominant magnetic carrier. An increase of κ with temperature up to 500 °C was observed and suggested a neoformation of magnetite as a result of thermal alteration of Fe-rich clay-minerals [40]. These alterations could be confirmed by the significantly elevated κ values (more than twofold) in cooling curves for temperatures <580 °C [41]. The increased susceptibility below 250 °C and the peaks around 250–300 °C is probably due to single domain (SD) or pseudo-single domain (PSD) particles becoming superparamagnetic (SP) at elevated temperatures [18,41,42]. A slight indication for hematite could be seen in dusts from Zhuzhou and Hezhang (Fig. 5b and c) due to the decreasing of κ during heating treatment between 600 and 700 °C [41]. However, an increase of κ with temperature between 600 and 700 °C was found in dusts from Ezhou (Fig. 5a). This may be explained by two possible reasons. One is due to the presence of metallic iron particles, which might undergo transformation from SD/PSD to SP. The other is attributed to a neoformation of metallic iron as a result of reduction of magnetite (Fe_3O_4) by carbon involved in the sample (deduced from the result of XRD, see below). This could be confirmed by the enhanced susceptibility in cooling curves for temperatures between 600 and 700 °C.

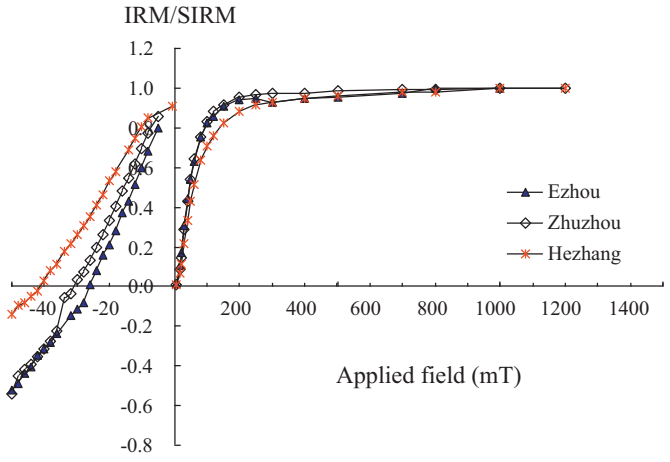

Fig. 3. Isothermal remanent magnetization (IRM) acquisition and back-field demagnetization curves for selected dust samples.

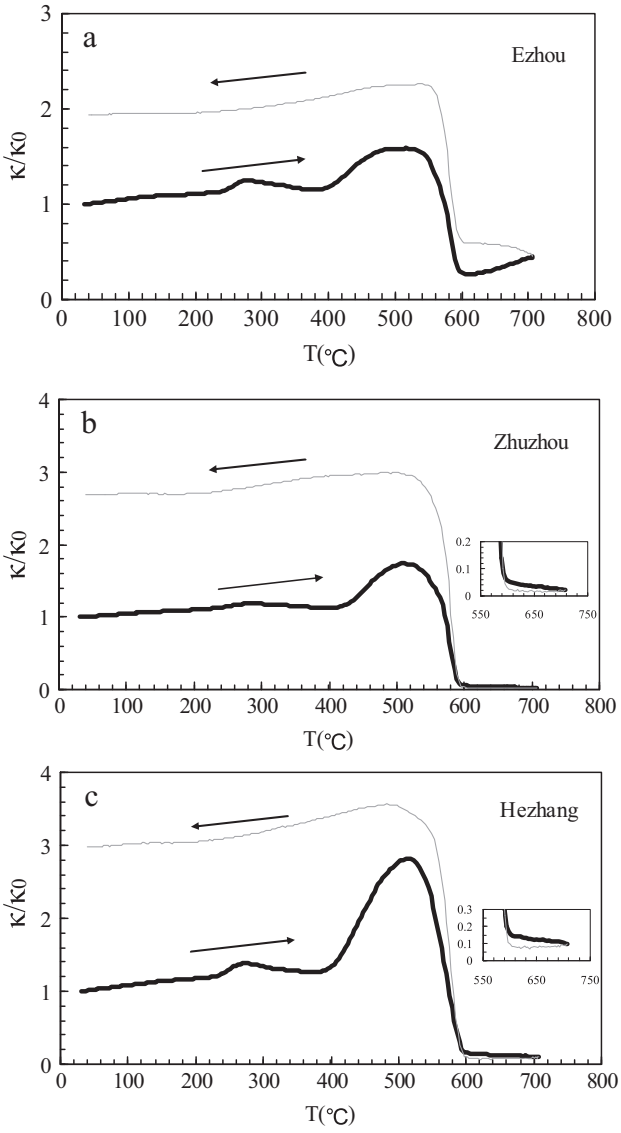

Fig. 4. Temperature-dependence of magnetic susceptibility (κ–T) heating (black line) and cooling (gray line) curves of selected dust samples. Each curve was normalized with its corresponding magnetic susceptibility at room temperature (κ_0).

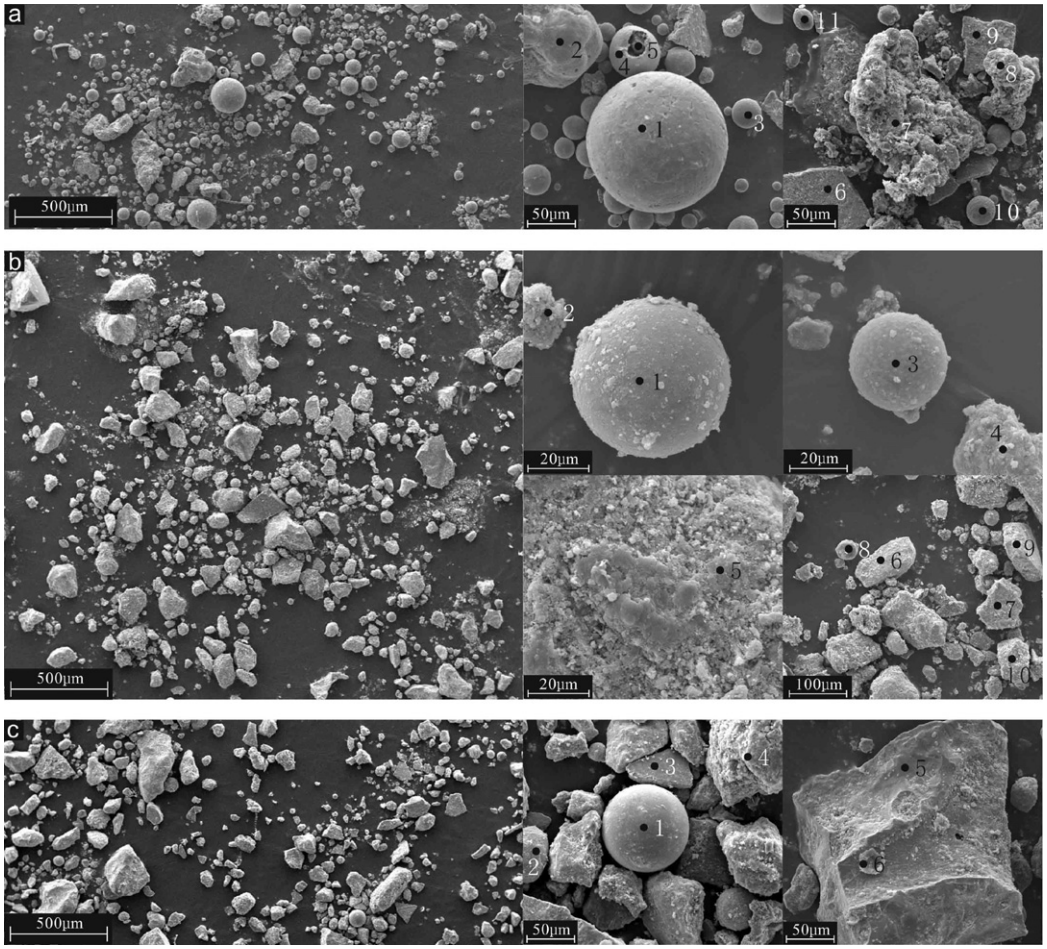

Fig. 5. SEM photographs of magnetic extracts from selected dust samples. (a) Ezhou, (b) Zhuzhou, and (c) Hezhang. The dark dots indicate the spots of EDX analysis.

The observations of environmental SEM of the extracts revealed two major groups of iron oxides, spherule and irregular shape, among the magnetic phase (Fig. 5). Magnetic particles in dust from Ezhou were dominated by spherules with grain sizes ranging from several to more than one hundred of micrometers (Fig. 5a). In some cases, a calcium core can be seen inside the spherules (Fig. 5a, point 5). EDX analysis revealed that the concentrations of Fe in these magnetic spherules were about 75%, whereas the rest irregular-shaped magnetic particles had a wider range of Fe concentrations (44.65–82.33%). Some of the irregular-shaped particles also contained substantial amounts of Cr and Mn (Fig. 5a, point 2 and 11 and Table 3). This is consistent with the results of chemical analysis (Table 1). On the contrary, magnetic particles in dust from Zhuzhou and Hezhang were mainly irregular shape with grain sizes up to 300 μm (Fig. 5b and c). Fe concentrations in these irregular particles varied greatly, from 9.10 to 73.86% and 11.47 to 83.73% for Zhuzhou and Hezhang, respectively (Table 3). However, small amounts of magnetic spherules can still be found in these samples. Moreover, the spherules from Zhuzhou had a saccharoidal surface (Fig. 5b, point 1 and 3) with high Al and Si contents (Table 3), probably indicating the existences of amorphous aluminum silicate coater [43]. The iron spherules are typical products of high temperature combustion, whilst the irregular-shaped particles and metallic iron are probably associated with the emission during NFM processing (e.g., shaping, cutting, and polishing the metal alloy) and the erosion of traffic parts.

X-ray diffraction analysis of magnetic extracts confirmed the findings of magnetic parameters. As shown in Fig. 6, magnetic extracts from Ezhou sample primarily consisted of magnetite (Fe_3O_4) but also small amounts of metallic iron. In addition, graphite could also be found in these extracts. However, magnetic minerals in samples from Zhuzhou and Hezhang were dominated by magnetite and small amounts of hematite.

3.3. Correlation analysis

The results of correlation analysis between different heavy metals are listed in Table 4. For dusts from Ezhou and Hezhang, most of the considered metals, except As and Cd, were correlated significantly with each other, indicating the common origins of heavy metals in each of the sample sets. Furthermore, the strong correlation between iron and the other heavy metals confirmed that iron hydroxides/oxides are important absorbers and carriers of heavy metals in these samples. In comparison with data from Ezhou and Hezhang, the correlations between different metals in dust from Zhuzhou were less significant. There were two groups of metals, As–Cd–Cu–Pb–Zn and Co–Cr–Ni–V, showed significant interrelationship, suggesting different sources of heavy metals in these samples. This finding may explain the poor correlation between iron and the other heavy metals because particles from different sources might have different iron to metal ratios. For example, the plots of iron versus Pb and Zn (Fig. 7) revealed that anthropogenic particles in dust from Zhuzhou were derived from at least two sources with significantly different Fe/Pb and Fe/Zn ratios. One had high Fe/Pb and Fe/Zn ratios up to 250 and 70, respectively, whereas the other had low Fe/Pb and Fe/Zn ratios down to 11 and 4, respectively.

Table 3
EDX analysis results of magnetic extracts from Ezhou, Zhuzhou, and Hezhang.

Sample	Location	Element weight (%)							
		Fe	C	O	Al	Si	Ca	Cr	Mn
Ezhou	1	80.68	5.21	9.51	0.63	0.79	0.16	0.32	0.59
	2	52.93	6.15	10.41	0.90	1.20	0.24	9.16	16.20
	3	75.77	7.25	12.79	0.61	0.81	0.15	0.23	0.39
	4	74.20	6.58	10.00	1.59	2.43	0.32	1.01	1.66
	5	18.94	3.31	23.22	3.06	5.80	40.84	0.70	0.64
	6	82.33	0.79	2.41	0.62	1.10	0.30	2.80	8.51
	7	65.98	6.66	17.93	0.59	3.20	1.38	0.29	0.68
	8	75.25	4.95	12.03	0.15	3.17	1.75	0.50	0.84
	9	70.58	7.44	8.58	1.45	4.80	0.78	3.75	0.54
	10	73.10	6.39	15.61	0.68	0.88	0.17	0.27	0.66
	11	44.65	16.89	13.85	3.12	4.11	0.41	7.96	5.34
Zhuzhou	1	27.01	7.09	24.89	10.65	26.43	1.35	0.30	0.21
	2	9.10	32.74	29.22	5.71	11.89	5.66	0.08	0.18
	3	18.42	8.92	23.62	8.88	24.92	2.18	0.12	0.43
	4	44.79	12.74	22.72	2.88	4.91	4.47	0.26	0.48
	5	5.90	11.92	26.27	5.68	23.57	17.25	0.25	0.14
	6	43.71	12.75	21.82	4.16	8.61	2.86	0.11	0.35
	7	53.70	7.87	12.64	4.33	13.85	1.59	0.19	0.47
	8	20.69	27.03	21.14	6.35	9.66	5.74	0.14	0.37
	9	60.13	9.28	21.88	1.67	2.25	0.62	0.10	0.51
	10	73.86	6.13	12.20	1.19	2.11	0.39	0.26	0.61
Hezhang	1	75.30	5.93	15.33	0.46	0.78	0.26	0.20	0.66
	2	68.70	7.08	17.78	1.22	0.96	0.38	0.16	0.30
	3	57.88	11.65	22.67	2.12	2.94	1.38		0.22
	4	11.47	22.86	22.58	6.12	11.17	19.59	0.57	0.91
	5	83.73	8.42	3.83	0.50	1.01	0.34	0.43	0.61
	6	29.43	42.87	13.00	2.03	3.52	1.55	0.23	0.38

Table 4
Pearson's correlation coefficients (r) between different heavy metals.

	As	Ba	Cd	Co	Cr	Cu	Fe	Mn	Ni	Pb	V
EZ (n = 22)											
Ba	0.224										
Cd	0.520*	0.245									
Co	0.060	0.663**	0.097								
Cr	0.089	0.578**	0.057	0.961**							
Cu	0.070	0.619**	0.070	0.977**	0.977**						
Fe	0.158	0.706**	0.125	0.954**	0.949**	0.967**					
Mn	0.079	0.669**	0.010	0.979**	0.958**	0.968**	0.961**				
Ni	0.062	0.660**	0.076	0.981**	0.956**	0.962**	0.936**	0.959**			
Pb	0.316	0.650**	0.392	0.572**	0.510*	0.600**	0.637**	0.551**	0.518*		
V	0.253	0.701**	0.235	0.954**	0.922**	0.945**	0.954**	0.939**	0.918**	0.733**	
Zn	0.404	0.782**	0.478*	0.774**	0.707**	0.749**	0.782**	0.752**	0.708**	0.744**	0.868**
ZZ (n = 43)											
Ba	0.094										
Cd	0.934**	0.096									
Co	−0.066	0.100	−0.013								
Cr	−0.196	0.157	−0.234	0.068							
Cu	0.868**	0.262	0.815**	0.013	0.067						
Fe	0.265	0.358*	0.276	0.105	0.366*	0.484**					
Mn	0.135	0.269	0.102	0.162	0.155	0.164	0.295				
Ni	−0.111	0.252	−0.054	0.578**	0.469**	0.159	0.539**	0.283			
Pb	0.966**	0.093	0.976**	−0.018	−0.156	0.859**	0.336*	0.134	−0.036		
V	0.140	0.275	0.285	0.330*	0.088	0.191	0.506**	0.295	0.498**	0.247	
Zn	0.888**	0.052	0.875**	−0.064	−0.245	0.797**	0.270	0.129	−0.106	0.893**	0.243
HZ (n = 26)											
Ba	0.044										
Cd	0.382	0.479*									
Co	0.168	0.772**	0.367								
Cr	0.123	0.716**	0.372	0.767**							
Cu	0.371	0.499**	0.448*	0.763**	0.667**						
Fe	0.347	0.818**	0.510**	0.916**	0.827**	0.795**					
Mn	0.061	0.789**	0.553**	0.668**	0.644**	0.528**	0.729**				
Ni	0.435*	0.621**	0.624**	0.794**	0.756**	0.833**	0.840**	0.591**			
Pb	0.581**	0.562**	0.470*	0.633**	0.628**	0.691**	0.733**	0.451*	0.729**		
V	0.043	0.775**	0.299	0.918**	0.715**	0.697**	0.852**	0.680**	0.782**	0.533**	
Zn	0.445*	0.591**	0.845**	0.457*	0.559**	0.470*	0.631**	0.614**	0.724**	0.554**	0.457*

* Significant level at $p < 0.05$ (two-tailed).
** Significant level at $p < 0.01$ (two-tailed).

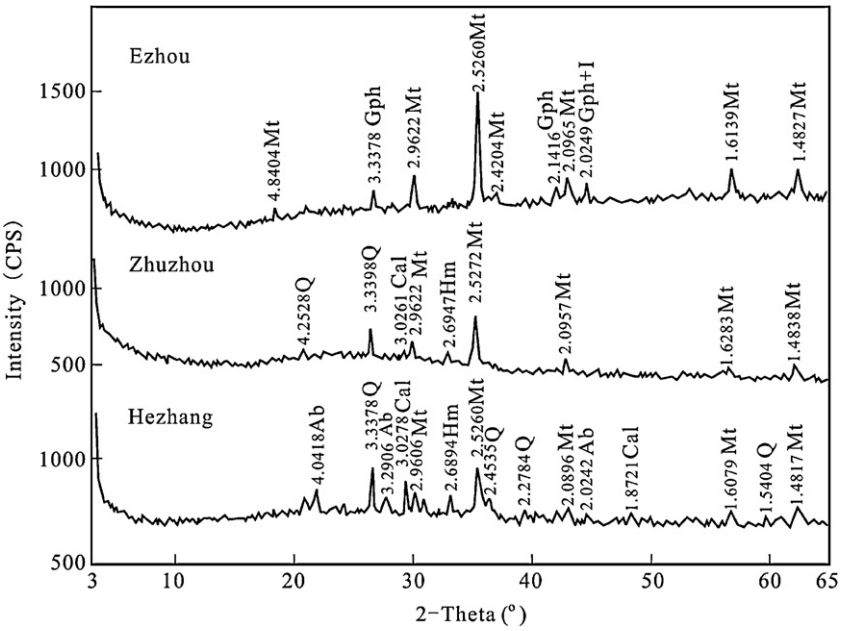

Fig. 6. X-ray diffraction pattern of magnetic extracts from selected dust samples. Mt – magnetite, Hm – hematite, I – iron, Gph – graphite, Q – quartz, Cal – calcite, Ab – albite.

Pearson correlation coefficients (r) between magnetic properties (χ and SIRM) and heavy metals are shown in Table 5. For dust from Hezhang, all heavy metals except As, as well as PLI, showed a strong positive correlation with χ and SIRM. For dust from Zhuzhou, χ was correlated significantly with Fe, Ba, Cr, Cu, Ni, and PLI, and SIRM was correlated significantly with Fe, Mn, Ba, Cr, Cu, Ni, Pb, V, and PLI. It should be noted that SIRM in dust from the two cities showed a better relationship with heavy metals (except Cr) than χ. This finding is in agreement with many of the previous studies [8,12,18,44] and suggests that SIRM is a more efficient indicator than χ for dust heavy metals due to the fact that anthropogenic emitted particles are generally ferrimagnetic minerals. On the contrary, no significant correlations were found between either χ or SIRM and heavy metals for samples from Ezhou. This may be explained by the presence of iron particles in the dust, which in minor amounts may have a great influence on the magnetic parameters [33] but not on the total iron concentrations. A similar result had been found in street dust from Loudi, China [35].

3.4. Implication for detecting environmental heavy metal contamination

The application of magnetic measurements to detecting heavy metal contamination is based on the relationship between magnetic parameters (mainly χ and SIRM) and heavy metals. This is controlled by two factors: the relationship between magnetic parameters and iron concentrations and the relationship between iron and heavy metals. Significant correlation between magnetic parameters and iron is widespread because anthropogenic emitted magnetic minerals are usually ferrimagnetic phases (iron hydroxides/oxides), which have an equal contribution to magnetic properties (χ and SIRM) and total iron concentration. However, this is not always the case. The results from Ezhou in this study indicate that the presence of iron particles (Figs. 4a and 6) could weaken the correlation between iron and magnetic parameters (Table 5) because even very low levels of iron particles can contribute to high magnetic susceptibility values [33,35]. Similarly, significant

Table 5
Pearson's correlation coefficients (r) between magnetic properties (χ and SIRM) and heavy metals.

	Ezhou (n = 22)		Zhuzhou (n = 43)		Hezhang (n = 26)	
	χ	SIRM	χ	SIRM	χ	SIRM
Fe	0.188	−0.223	0.884**	0.942**	0.914**	0.928**
Mn	0.133	−0.191	0.254	0.346*	0.648**	0.698**
As	0.072	−0.206	0.185	0.273	0.354	0.331
Ba	−0.129	−0.230	0.383*	0.417**	0.711**	0.736**
Cd	−0.022	0.004	0.167	0.264	0.442*	0.486*
Co	0.119	−0.195	0.035	0.026	0.838**	0.871**
Cr	0.213	−0.099	0.589**	0.448**	0.789**	0.770**
Cu	0.171	−0.90	0.441**	0.526**	0.686**	0.710**
Ni	0.165	−0.216	0.479**	0.470**	0.707**	0.751**
Pb	−0.202	−0.208	0.259	0.346*	0.706**	0.709**
V	0.070	−0.209	0.248	0.353*	0.662**	0.722**
Zn	−0.160	−0.269	0.160	0.255	0.541**	0.565**
PLI	0.070	−0.232	0.478**	0.582**	0.838**	0.869**

* Significant level at $p < 0.05$ (two-tailed).
** Significant level at $p < 0.01$ (two-tailed).

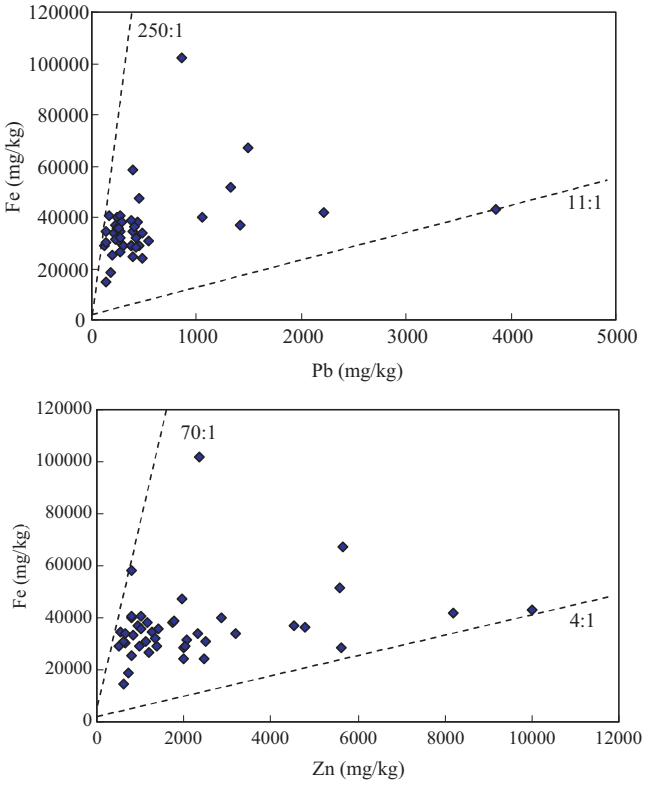

Fig. 7. Correlation scatter diagram between Fe and Pb, Zn.

correlation between iron and heavy metals has often been found in various environmental samples, such as the results from Ezhou and Hezhang in the present study (Table 4). However, this relationship is influenced by the diversity of anthropogenic emission sources. Significant correlation between iron and heavy metals is generally found in pollutants from single sources (e.g., results from Ezhou and Hezhang), whereas multi-sources of pollutants usually have poor coefficients of iron with heavy metals (e.g., results from Zhuzhou). Therefore, our study demonstrates that it is difficult to accurately evaluate the degree of heavy metal contamination by magnetic concentration if metallic iron particles and multi-sources of pollutants are present. Nevertheless, magnetic concentration is sensitive to the total load of heavy metal contaminants. For example, the highest χ and SIRM in dusts from Ezhou are clearly a response to high concentrations of heavy metals in this area (Table 1). This demonstrates that in many cases the magnetic method is a reliable and powerful technique to detect and outline target regions with possible higher heavy metal contamination.

4. Conclusion

The present study demonstrates a common coexistence of magnetic particles and heavy metals in dusts from three NFM smelting/processing impacted cities. Two shapes of magnetic particles, spherule and angular-shaped particles, were identified by the SEM-EDX analysis. Mineralogical analyses indicate that the magnetic particles from Ezhou were dominated by magnetite and metallic iron, whereas those from Zhuzhou and Hezhang were consisted of magnetite and hematite. The relationship between magnetic parameters (χ and SIRM) and heavy metals varied among different cities, depending on the presence of iron particles and multi-sources of metal pollutants in the samples. Our study demonstrates that magnetic parameters in dusts are sensitive to the NFM smelting/processing related heavy metal pollutants and thus can be used as a powerful proxy to detect and outline target regions with possible higher heavy metal contamination.

Acknowledgments

We are grateful to the two reviewers for their useful suggestions and comments of this study. This study was financial supported by the Natural Science Foundation of China (40904015, 40903041, and 41273003).

References

[1] N.V. Jordanova, D.V. Jordanova, L. Veneva, K. Yorova, E. Petrovsky, Magnetic response of soils and vegetation to heavy metal pollution – a case study, Environ. Sci. Technol. 37 (2003) 4417–4424.
[2] C. Spiteri, V. Kalinski, W. Rösler, V. Hoffmann, E. Appel, Magnetic screening of a pollution hotspot in the Lausitz area, Eastern Germany: correlation analysis between magnetic proxies and heavy metal contamination in soils, Environ. Geol. 49 (2005) 1–9.
[3] T. Yang, Q. Liu, L. Chan, G. Cao, Magnetic investigation of heavy metals contamination in urban topsoils around the East Lake, Wuhan, China, Geophys. J. Int. 171 (2007) 603–612.
[4] A. Kapička, E. Petrovský, H. Fialová, V. Podrázský, I. Dvořák, High resolution mapping of anthropogenic pollution in the Giant Mountains National Park using soil magnetometry, Stud. Geophys. Geod. 52 (2008) 271–284.
[5] A. Blundell, J.A. Hannam, J.A. Dearing, J.F. Boyle, Detecting atmospheric pollution in surface soils using magnetic measurements: a reappraisal using an England and Wales database, Environ. Pollut. 157 (2009) 2878–2890.
[6] O. Rosowiecka, J. Nawrocki, Assessment of soils pollution extent in surroundings of ironworks based on magnetic analysis, Stud. Geophys. Geod. 54 (2010) 185–194.
[7] W. Kim, S.J. Doh, Y. Yu, Anthropogenic contribution of magnetic particulates in urban roadside dust, Atmos. Environ. 43 (2009) 3137–3144.
[8] T. Yang, Q. Liu, H. Li, Q. Zeng, L. Chan, Anthropogenic magnetic particles and heavy metals in the road dust: magnetic identification and its implications, Atmos. Environ. 44 (2010) 1175–1185.
[9] M.S. Bućko, T. Magiera, L.J. Pesonen, B. Janus, Magnetic, geochemical, and microstructural characteristics of road dust on roadsides with different traffic volumes a case study from Finland, Water Air Soil Pollut. 209 (2010) 295–306.
[10] M.S. Bučko, T. Magiera, B. Johanson, E. Petrovský, L.J. Pesonen, Identification of magnetic particulates in road dust accumulated on roadside snow using magnetic, geochemical and micro-morphological analyses, Environ. Pollut. 159 (2011) 1266–1276.
[11] Q. Qiao, C. Zhang, B. Huang, J.D.A. Piper, Evaluating the environmental quality impacted of the 2008 Beijing Olympic Games: magnetic monitoring of street dust in Beijing Olympic Park, Geophys. J. Int. 187 (2011) 1222–1236.
[12] G. Wang, F. Oldfield, D. Xia, F. Chen, X. Liu, W. Zhang, Magnetic properties and correlation with heavy metals in urban street dust: a case study from the city of Lanzhou, China, Atmos. Environ. 46 (2012) 289–298.
[13] M.A.E. Chapparro, J.C. Bidegain, A.M. Sinito, S.S. Jurado, C.S.G. Gogorza, Relevant magnetic parameters and heavy metals from relatively polluted stream sediments – vertical and longitudinal distribution along a cross-city stream in Buenos Aires Province, Argentina, Stud. Geophys. Geod. 48 (2004) 615–636.
[14] T. Yang, Q. Liu, L. Chan, L. Chan, Z. Liu, Magnetic signature of heavy metals pollution of sediments: case study from the East Lake in Wuhan, China, Environ. Geol. 52 (2007) 1639–1650.
[15] W. Zhang, L. Yu, M. Lu, S.M. Hutchinson, H. Feng, Magnetic approach to normalizing heavy metal concentrations for particle size effects in intertidal sediments in the Yangtze Estuary, China, Environ. Pollut. 147 (2007) 238–244.
[16] M.L. Rijal, E. Appel, E. Petrovský, U. Blaha, Change of magnetic properties due to fluctuations of hydrocarbon contaminated groundwater in unconsolidated sediments, Environ. Pollut. 158 (2010) 1756–1762.
[17] S. Bijaksana, E.K. Huliselan, Magnetic properties and heavy metal content of sanitary leachate sludge in two landfill sites near Bandung, Indonesia, Environ. Earth Sci. 60 (2010) 409–419.
[18] C. Zhang, Q. Qiao, J.D.A. Piper, B. Huang, Assessment of heavy metal pollution from a Fe-smelting plant in urban river sediments using environmental magnetic and geochemical methods, Environ. Pollut. 159 (2011) 3057–3070.
[19] J. Matzka, B.A. Maher, Magnetic biomonitoring of roadside tree leaves: identification of spatial and temporal variations in vehicle-derived particulates, Atmos. Environ. 33 (1999) 4565–4569.
[20] A.F. Davila, D. Rey, K. Mohamed, B. Rubio, A.P. Guerra, Mapping the sources of urban dust in a coastal environment by measuring magnetic parameters of *Platanus hispanica* leaves, Environ. Sci. Technol. 40 (2006) 3922–3928.
[21] C. Zhang, B. Huang, Z. Li, H. Liu, Magnetic properties of highroad-side pine tree leaves in Beijing and their environmental significance, Chin. Sci. Bull. 51 (2006) 3041–3052.

[22] B.A. Maher, C. Moore, J. Matzka, Spatial variation in vehicle-derived metal pollution identified by magnetic and elemental analysis of roadside tree leaves, Atmos. Environ. 42 (2008) 364–373.
[23] H. Salo, M.S. Bućko, E. Vaahtovuo, J. Limo, J. Mäkinen, L.J. Pesonen, Biomonitoring of air pollution in SW Finland by magnetic and chemical measurements of moss bags and lichens, J. Geochem. Explor. 115 (2012) 69–81.
[24] H.A. Roels, J-P. Buchet, R.R. Lauwerys, P. Bruaux, F. Claeys-Thoreau, A. Lafontaine, G. Verduyn, Exposure to lead by the oral and the pulmonary routes of children living in the vicinity of a primary lead smelter, Environ. Res. 22 (1980) 81–94.
[25] L. Ferreira-Baptista, E. De Miguel, Geochemistry risk assessment of street dust in Luanda, Angola: a tropical urban environment, Atmos. Environ. 39 (2005) 4501–4512.
[26] N. Zheng, J. Liu, Q. Wang, Z. Liang, Health risk assessment of heavy metal exposure to street dust in the zinc smelting district, Northeast of China, Sci. Total Environ. 408 (2010) 726–733.
[27] M.F. Soto-Jiménez, A.R. Flegal, Childhood lead poisoning from the smelter in Torreón, México, Environ. Res. 111 (2011) 590–596.
[28] B.A. Maher, A. Alekseev, T. Alekseeva, Magnetic mineralogy of soils across the Russian steppe: climatic dependence of pedogenic magnetic formation, Palaeogeogr. Palaeoclimatol. Palaeoecol. 201 (2003) 321–341.
[29] G. Müller, Index of geoaccumulation in sediments of the Rhine River, Geojournal 2 (1969) 108–118.
[30] E. Angulo, The Tomlinson pollution load index applied to heavy metal Mussel-Watch data: a useful index to assess coastal pollution, Sci. Total Environ. 187 (1996) 19–56.
[31] A.K. Singh, S.I. Hasnain, D.K. Banerjee, Grain size and geochemical portioning of heavy metals in sediments of the Danodar River e a tributary of the lower Ganga, India, Environ. Geol. 39 (2003) 90–98.
[32] F. Oldfield, Environmental magnetism – a personal perspective, Quarter. Sci. Rev. 10 (1991) 73–85.
[33] C. Zhang, Q. Liu, B. Huang, Y. Su, Magnetic enhancement upon heating of environmentally polluted samples containing haematite and iron, Geophys. J. Int. 181 (2010) 1381–1394.
[34] J.A. Dearing, K.L. Hay, S.M.J. Baban, A.S. Huddleston, E.M.H. Wellington, P.J. Loveland, Magnetic susceptibility of soil: an evaluation of conflicting theories using a national data set, Geophys. J. Int. 127 (1996) 728–734.
[35] C. Zhang, Q. Qiao, E. Appel, B. Huang, Discriminating sources of anthropogenic heavy metals in urban street dusts using magnetic and chemical methods, J. Geochem. Explor. 119-120 (2012) 60–75.
[36] P. Li, X. Qiang, Y. Tang, C. Fu, X. Xu, X. Li, Magnetic susceptibility of the dust of street in Xi'an and the implication on pollution, China Environ. Sci. (in Chinese) 30 (2010) 309–314.
[37] M.K. Chan, L.S. Chan, S.L. Ng, Q.S. Liu, Heavy metal contents and magnetic properties of street dust in two districts of different traffic density in Hong Kong, Geophys. Solut. Environ. Eng. 1–2 (2006) 807–811.
[38] W. Kim, S.J. Doh, Y.H. Park, S.T. Yun, Two-year magnetic monitoring in conjunction with geochemical and electron microscopic data of roadside dust in Seoul, Korea, Atmos. Environ. 41 (2007) 7627–7641.
[39] S.J. Xie, J.A. Dearing, J. Bloemendal, The organic matter content of street dust in Liverpool, UK, and its association with dust magnetic properties, Atmos. Environ. 34 (2000) 269–275.
[40] C.X. Zhang, G.A. Paterson, Q.S. Liu, A new mechanism for the magnetic enhancement of hematite during heating: the role of clay minerals, Stud. Geophys. Geod. 56 (2012) 845–860.
[41] T. Yang, Q. Zeng, Z. Liu, Q. Liu, Magnetic properties of the road dusts from two parks in Wuhan city, China: implications for mapping urban environment, Environ. Monit. Assess. 177 (2011) 637–648.
[42] S.R. Goddu, E. Appel, D. Jordanova, F. Wehland, Magnetic properties of road dust from Visakhapatnam (India) – relationship to industrial pollution and road traffic, Phys. Chem. Earth 29 (2004) 985–995.
[43] T. Magiera, M. Jabłońska, Z. Strzyszcz, M. Rachwal, Morphological and mineralogical forms of technogenic magnetic particles in industrial dusts, Atmos. Environ. 45 (2011) 4281–4290.
[44] Z. Zhu, Z. Han, X. Bi, W. Yang, The relationship between magnetic parameters and heavy metal contents of indoor dust in e-waste recycling impacted area, Southeast China, Sci. Total Environ. 433 (2012) 302–308.